15th IFK
Proc. of the 15th International Fluid Power Conference <Symposium/Conference>
<DOI>

A PID Controller Gain Adjustment Mechanism to Balance EHA Tracking and Health

Simo Käki, Mikko Huova, Tatiana Minav

Innovative Hydraulics and Automation, Tampere University, Tampere, Finland, firstname.lastname@tuni.fi

Abstract.

Electro-hydraulic systems power much of today's working machinery, which often operate in remote or harsh locations where maintenance is difficult. Given the cost and safety concerns of unplanned outages, strategies that prevent breakdowns between service intervals are crucial. One prominent approach is to adjust the parameters of existing controllers in a health-aware manner to potentially extend the remaining useful life (RUL) of the components.

Consequently, this paper presents a health-aware adjustment method for a PID-controlled electro-hydrostatic actuator that tunes the controller gain online to balance tracking and health. The method estimates a hidden degradation state using an extended Kalman filter and models the short-horizon degradation as a Wiener process. It derives an inverse-Gaussian RUL distribution from the degradation estimates and fits a ridge model that links control effort to degradation rate. Moreover, a supervisory cost function weighs an integral-squared error against a soft health constraint and selects gain updates accordingly.

In accelerated simulation studies, an update of the controller gain slowed degradation and thus extended the RUL. The system met a 95 percent survival target while keeping the control error modest. This approach adds improved life-extension potential with minimal architectural change, and it can run as a cloud-based supervisory layer that updates parameters using recorded data.

Keywords. Electro-hydrostatic actuator, external gear pump, health-aware control, PID-control, remaining useful life

1. INTRODUCTION

Maintaining working machinery is crucial, as the cost of unplanned outages can be significant. However, this is often challenging in practice, since machines frequently operate in remote and harsh environments. Accurate remaining useful life (RUL) prediction can provide key information for maintenance scheduling. In recent years, estimating the RUL of various components in electro-hydraulic systems has seen considerable research interest. Bejaoui et al. [1] and Dahal et al. [2] investigated the RUL of rotating machines using data-driven methods. On the hydraulic side, the pump has been the focus of multiple papers utilizing physics-based approaches [3, 4], data-based approaches [5–7], or a combination of these, i.e., hybrid approaches [8, 9], to estimate the RUL.

Previous research has tended to focus on RUL prediction and fault-tolerant control rather than on failure prevention [10–13]. However, there has been growing interest in life-extending control or health-aware control (HAC) for systems that are difficult to maintain [14–16]. A recent survey by Zagorowska et al. [17] highlights the potential of HAC and underlines the need for more research that integrates degradation-dependent models in simulations when validating optimization and scheduling layers.

A regulatory control system requires accurate knowledge of the system behavior over short timescales. In contrast, degradation is often a very slow process and depends on the way in which the system is operated as well as on external factors. Thus, integrating both the performance and degradation mitigation in the same control loop leads inevitably to computational problems [18]. This problem naturally leads to a multi-layer approach where a long-run RUL problem is solved separately from the lower-level regulatory problem.

The aim of this paper is to develop an adjustment method for a proportional-integral-derivative (PID) controller in an electro-hydrostatic actuator (EHA) system. The EHA is selected, as it combines tight servo performance with compact, self-contained hydraulics. Moreover, the adoption of EHAs is anticipated to increase substantially with the growing introduction of electrification of working machinery and aerospace applications [19].To enable RUL-extending capabilities, measurements of oil flow, pressures, and pump rotational speed are required. This approach provides an alternative to complex HAC systems by adjusting the existing controller rather than designing degradation-aware control from scratch. This has the added benefit that the adjustment mechanism can be executed as a cloud-based service. Additionally, minimal assumptions are made about the hidden degradation model of the gear pump in the degradation estimation step.

The remainder of this paper is structured into four sections. Section 2 outlines the methodology applied throughout the study. Section 3 introduces the simulation model and explains the techniques. Section 4 discusses the main results in detail, and Section 5 concludes with a summary of the key findings and their relevance to fluid power applications.

2. METHODOLOGY

2.1. Degradation Model

In this paper, the RUL optimization is called the adjustment mechanism, which updates the parameters of the regulatory controller. To simulate the behavior of an adjustment mechanism, accurate knowledge of the degradation is needed. A single-input single-output (SISO) system with degrading actuator is considered. Here, the time-varying and hidden degradation variable is defined $\phi(t)$. To model the evolution of the degradation, a nonlinear Wiener process model is employed [19–21] with the following equation:

$$\phi(t) = \phi_0 + \int_0^t \varphi(\tau, \boldsymbol{\theta}, \dots) d\tau + \sigma B(t), \tag{1}$$

where ϕ_0 is the initial value, $\varphi(\tau, \boldsymbol{\theta}, \dots)$ is the deterministic nonlinear function of τ with the parameter vector $\boldsymbol{\theta}$ and possible other inputs that describe the degradation rate, σ is the diffusion parameter which reflects the degradation variation, and $B(t)$ is the standard Brownian motion.

The deterministic part of Equation (1) is often coupled with the state, inputs, and/or outputs of the actuator, making this a factor-based model. This coupling is heavily content dependent, and a considerable amount of research has been conducted to investigate suitable formulations [17].

The degradation variable represents the strength of an item. The item fails when the process reaches an adverse threshold state for the first time. In this case, the lifetime in component-level prognostics is usually defined as the first hitting time (FHT) of the degradation process reaching a failure threshold ϕ_f [23], which is denoted as

$$t_f = \inf\{t \geq 0 : \phi(t) \geq \phi_f \mid \phi(0) < \phi_f\}, \tag{2}$$

where t_f is the failure time. Here, it is worth noting that the above definition is only applicable to a case with an increasing degradation process. Additionally, the choice of failure threshold is not obvious. Thus, careful engineering knowledge of the system requirements should be used to determine a sufficient value.

Differentiating Equation (1) yields

$$\frac{d}{dt}\phi(t) = \varphi(t, \boldsymbol{\theta}, \dots) + \sigma w(t), \tag{3}$$

where $w(t) \sim \mathcal{N}(0,1)$ is white noise. The degradation rate $\varphi(\dots)$ is often quite slow, so it is safe to assume that an average rate gives a reasonable estimate of the immediate future degradation behavior. This assumption holds when the variation in the degradation rate over time is negligible, making the average rate particularly suitable for short-term prediction. Otherwise, a time-dependent rate should be considered for improved accuracy. Following this assumption, the nonlinear degradation model (1) can be estimated with the linear Wiener process model

$$\phi(t) \approx \phi_0 + \mu t + \sigma B(t), \tag{4}$$

where μ is the (constant) degradation rate. This simplification can be improved with historical knowledge of degradation progression.

2.2. Extended Kalman Filter

An extended Kalman filter (EKF) is a nonlinear state estimation technique that extends the classical Kalman filter to systems with nonlinear dynamics and/or measurement models [24]. By linearizing the system around the current estimate with first-order Taylor expansion, the EKF enables recursive estimation of the system state in real time. This makes the EKF an effective choice for estimating the current degradation rate in addition to the current degradation. To achieve this, Equation (4) is written as

$$\begin{bmatrix} \dot{\mu} \\ \dot{\phi} \end{bmatrix} = \begin{bmatrix} 0 & 0 \\ 1 & 0 \end{bmatrix} \begin{bmatrix} \mu \\ \phi \end{bmatrix} + w, \tag{5}$$

where $w \sim \mathcal{N}(0, \Sigma_w)$ is the process noise with a zero-mean Gaussian distribution and $\boldsymbol{x}_{kf} = [\mu \quad \phi]^{\mathrm{T}}$ is the state vector. Equation (5) should be supplemented with (possibly) the nonlinear measurement function

$$\boldsymbol{y}_{kf} = h(\boldsymbol{x}_{kf}, \boldsymbol{u}_{kf}) + v, \tag{6}$$

where $v \sim \mathcal{N}(0, \Sigma_v)$ is the measurement noise with a zero-mean Gaussian distribution that relates the degradation $\phi(t)$ to the measured values $\boldsymbol{y}_{kf}$ and inputs $\boldsymbol{u}_{kf}$.

The EKF algorithm consists of a prediction step and an update step. In the prediction step, the state and covariance are propagated forward in time using the system model. This *a priori* information is denoted by a superscript minus sign ($^-$). In the update step *a posteriori* information is denoted by a superscript plus sign ($^+$).

The EKF algorithm requires the Jacobians of the system dynamics and measurement functions. For the case of Equation (5), the discrete time Jacobians are

$$F = \begin{bmatrix} 1 & 0 \\ t_{s,ekf} & 1 \end{bmatrix}, \tag{7}$$

$$H = \frac{\partial}{\partial \boldsymbol{x}_{kf}} h(\boldsymbol{x}_{kf}, \boldsymbol{u}_{kf}), \tag{8}$$

where $t_{s,ekf}$ is the sampling time of the filter. These are then utilized in the prediction step to update the state estimate and covariance with equations

$$\hat{\boldsymbol{x}}_{kf}^{-}[k] = F \hat{\boldsymbol{x}}_{kf}^{+}[k-1], \tag{9}$$

$$\Sigma_{\boldsymbol{x}}^{-}[k] = F \Sigma_{\boldsymbol{x}}^{+}[k-1] F^{\mathrm{T}} + \Sigma_w, \tag{10}$$

where k is the current sampling timestep.

The update step starts with calculating the *a priori* measurements

$$\hat{\boldsymbol{y}}_{kf}^{-}[k] = h(\hat{\boldsymbol{x}}_{kf}^{-}[k], \boldsymbol{u}_{kf}[k]), \tag{11}$$

and the Kalman gain

$$K = \Sigma_{\boldsymbol{x}}^{-}[k] H^{\mathrm{T}} (H \Sigma_{\boldsymbol{x}}^{-}[k] H^{\mathrm{T}} + \Sigma_v)^{-1}. \tag{12}$$

The *a priori* measurements and the Kalman gain are then used to update the state estimate

$$\hat{\boldsymbol{x}}_{kf}^{+}[k] = \hat{\boldsymbol{x}}_{kf}^{-}[k] + K(\boldsymbol{y}_{kf}[k] - \hat{\boldsymbol{y}}_{kf}^{-}[k]). \tag{13}$$

Finally, the covariance matrix is updated with the Joseph form

$$\Sigma_{\boldsymbol{x}}^{+}[k] = (I - KH) \Sigma_{\boldsymbol{x}}^{-}[k] (I - KH)^{\mathrm{T}} + K \Sigma_v K^{\mathrm{T}}, \tag{14}$$

where I is the identity matrix of a necessary size. The use of the Joseph form prevents the loss of positive definiteness in the covariance matrix due to numerical errors. This formulation is crucial when dealing with small numerical updates in long-term estimation tasks. Moreover, this formulation of the EKF enables an estimate of the degradation and the drift of a wide range of components. However, there are limits, which are outside the scope of this paper, as to the extent to which EKF can be utilized in this manner.

2.3. RUL Estimation

To estimate the RUL of the component, the remaining degradation margin is calculated with

$$L = \phi_f - \hat{\phi}[k], \tag{15}$$

where $\hat{\phi}[k]$ is the current degradation estimate from the EKF. For a meaningful prognostic horizon, $L > 0$ is required. Utilizing the slow degradation assumption in Equation (4), the RUL for this process becomes a classical FHT problem. For Brownian motion with a positive drift, the FHT to a fixed level has an inverse Gaussian (IG) distribution [23]. This link between drifted Brownian motion and the IG law is a standard result in stochastic process theory and is widely used in degradation-based reliability modeling.

In particular, if L is the distance to the failure threshold, then

$$\hat{t}_{RUL} \sim \mathrm{IG}\left(\frac{L}{\mu}, \frac{L^2}{\sigma^2}\right). \tag{16}$$

The corresponding cumulative distribution function (CDF) can be written using the standard normal distribution $\Phi(\cdot)$

$$F_{IG}(t) = \Phi\left(\frac{\hat{\mu}t - L}{\hat{\sigma}\sqrt{t}}\right) + \exp\left(\frac{2\hat{\mu}L}{\hat{\sigma}^2}\right)\Phi\left(-\frac{\hat{\mu}t + L}{\hat{\sigma}\sqrt{t}}\right), \tag{17}$$

where $\hat{\mu}$ is the current drift estimate and $\hat{\sigma}$ is the current diffusion estimate.

For a stable estimate of RUL, an evaluation time with a moving average can be utilized. As the EKF estimates the degradation with a low sampling time, a variety of unwanted dynamics and noise can negatively impact the calculations. At every evaluation time t_{eval}, the average from a recent data window for $\hat{\mu}$ can be calculated. Accordingly, the current diffusion estimate measures the random variability of degradation that is not explained by the drift estimate. The maximum likelihood estimate for the diffusion can be calculated with

$$\hat{\sigma}^2 = \frac{1}{\sum t_s} \sum_k \frac{(\boldsymbol{\phi}_W[k] - \boldsymbol{\phi}_W[k-1] - \hat{\mu}t_s)^2}{t_s}, \tag{18}$$

where $\boldsymbol{\phi}_W$ is the vector of degradation estimates from the EKF with the length of the moving window. For numerical stability, it is recommended to normalize $\hat{\phi}$ and $\hat{\mu}$ by dividing them with the failure threshold.

Finally, the mean RUL can be calculated with

$$\hat{t}_{RUL} = \frac{L}{\hat{\mu}}. \tag{19}$$

For a more conservative estimate, a survival percentage can be chosen (i.e., 95%). Then, the RUL must be solved from

$$F_{IG}(\hat{t}_{RUL,p}) = 1 - p, \tag{20}$$

where p is the survival probability.

The RUL estimate is visualized in Figure 2.1. The Figure 2.1 (a) shows the recent degradation estimate date from the EKF and the failure threshold. Then, the model from Equation (4) is fitted to this data and plotted forward in time with a 3σ-band to show the uncertainty. The IG probability density function (PDF) from Figure 2.1 (b) is also plotted in Figure 2.1 (a). In Figure 2.1 (b), the mean RUL and the more conservative 95% survival RUL are plotted with vertical lines.

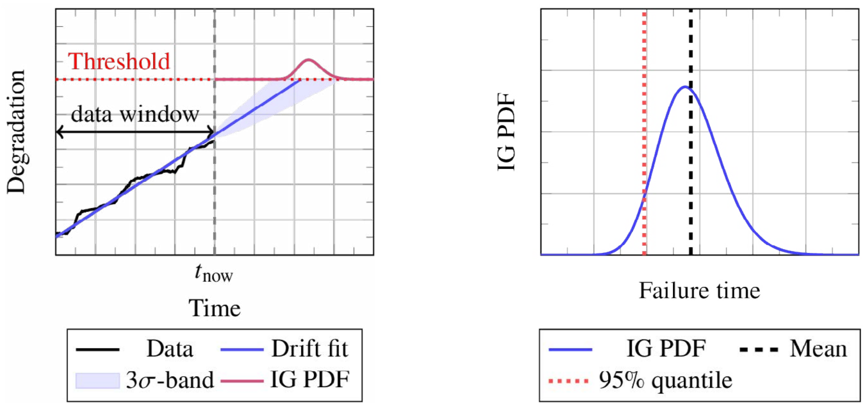

(a) **(b)**

Figure 2.1: Visualization of the RUL estimation from buffered data. (a) Drift fit to recent degradation data. (b) IG PDF with $\hat{t}_{RUL}$ and $\hat{t}_{RUL,95\%}$.

2.4. Adjustment Mechanism

The adjustment mechanism requires information on the effect of the control signal $u(t)$ on the degradation speed. A simple linear model

$$\hat{\mu} \approx X\boldsymbol{\beta}, \tag{21}$$

where X is the feature matrix and $\boldsymbol{\beta}$ is the fitted coefficients of the model, can be fitted to buffered degradation rate estimates $\hat{\mu}$ from the EKF. The fitting can be achieved using ridge regression [25]. In this study, the features are chosen as constant, rotational speed, and rotational acceleration. The corresponding drift term becomes $\hat{\mu}(t) \approx \beta_0 + \beta_1 u(t) + \beta_2 \dot{u}(t)$. These features were selected to be consistent with the deterministic degradation contributions in later Equations (34) and (35), and because $u(t)$ is the only variable the controller can directly influence, making it the most relevant regressor for analyzing how control actions correlate with degradation speed in this framework.

More generally, degradation can also depend on exogenous and operating-condition variables such as pressure, temperature, and contamination level. Such variables can be appended as additional columns in X when reliable measurements are available. However, they are not included here because the present study focuses on a simplified simulation setting and isolates the influence of the control action.

It is assumed that the controlled system can be presented as a SISO discrete time linear state-space model

$$\boldsymbol{x}_p[k+1] = A_d\boldsymbol{x}_p[k] + B_d u[k], \tag{22}$$

$$y[k] = C_d\boldsymbol{x}_p[k] + D_d u[k], \tag{23}$$

where $\boldsymbol{x}_p$ is the state vector, A_d is the dynamics matrix, B_d is the input matrix, C_d is the output matrix, and D_d is the feedthrough matrix. The system output y is controlled by discrete 2DOF-PID controller of the form [26]

$$x_{f,2}[k] = q_1 x_{f,2}[k-1] + q_2\Big(\big(cr[k] - y[k]\big) - x_{f,1}[k-1]\Big), \tag{24}$$

$$x_{f,1}[k] = x_{f,1}[k-1] + t_s x_{f,2}[k], \tag{25}$$

$$u[k] = k_p\big(br[k] - y[k]\big) + u_i[k] - k_p t_d x_{f,2}[k], \tag{26}$$

$$u_i[k+1] = u_i[k] + \frac{k_p t_s}{t_i}\big(r[k] - y[k]\big), \tag{27}$$

where r is the target value for y, $x_{f,1}$ and $x_{f,2}$ are the states of a lowpass filter, k_p is the controller gain, t_i is the integral time, t_d is the derivative time, t_s is the sampling time, b is the proportional reference weight, and c is the derivative reference weight. The internal gains of the lowpass filter are calculated with

$$q_1 = \frac{\tau_f^2}{\tau_f^2 + 2t_s\tau_f + 2t_s^2}, \tag{28}$$

$$q_2 = \frac{2t_s}{\tau_f^2 + 2t_s\tau_f + 2t_s^2}, \tag{29}$$

where τ_f is the filter time constant.

Finally, the adjustment mechanism can be formulated as

$$\min_{k_p} J(k_p) \text{ such that } k_{p,min} < k_p < k_{p,max}, \tag{30}$$

where $J(k_p)$ is the cost function that relates the performance and RUL of the system to the controller gain k_p. To ensure dimensional consistency and allow tuning of priorities, the cost function is formulated as

$$J(k_p) = w_1 \cdot ISE(k_p) + w_2 \cdot HEALTH(k_p), \tag{31}$$

where w_1 and w_2 are weighting factors that balance tracking and health preservation, $ISE(k_p)$ is the integral squared error that can be calculated from the past reference values and simulated with Equations (22)–(27) and $HEALTH(k_p)$ is the health constraint. The health constraint is formulated as a soft constraint

$$HEALTH(k_p) = \begin{cases} 0 & \text{if } \hat{t}_{RUL,95\%}\big(\hat{\mu}(k_p)\big) \geq t_{RUL,req} \\ 10^6\Big(t_{RUL,req} - \hat{t}_{RUL,95\%}\big(\hat{\mu}(k_p)\big)\Big)^2 & \text{otherwise} \end{cases}, \tag{32}$$

where $t_{RUL,req}$ is the remaining mission time, $\hat{t}_{RUL,95\%}(\hat{\mu})$ is the 95% quantile RUL from Equation (20), and $\hat{\mu}(k_p)$ is the degradation rate from Equation (21), where the feature matrix can be constructed from the simulation.

The complete framework for the adjustment mechanism is presented in Figure 2.2. The extended Kalman filter is utilized to estimate the degradation and degradation rate from the rotation speed, generated flow, and port pressures of the pump. From these, a RUL estimate can be made. The degradation rate is used in the feature extraction block to estimate how the rotational speed affects the degradation speed. Finally, the optimizer employs this information to find the best value for the controller gain.

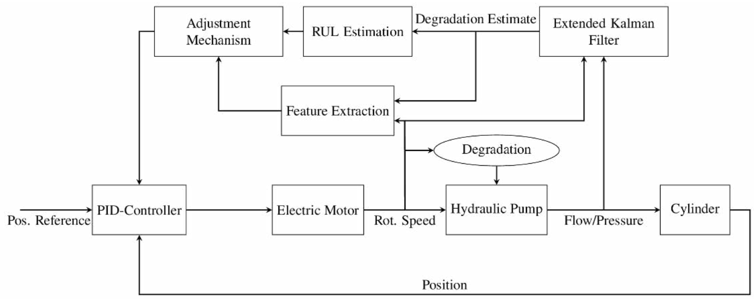

Figure 2.2: PID-controlled EHA with prognostics and health monitoring system connected to the adjustment mechanism to schedule the PID parameters.

3. SIMULATION MODEL

A Simulink model of an EHA system is used to evaluate the effectiveness of the adjustment mechanism. The whole simulation model is presented in more detail in a previous publication [27]. This section focuses on the main differences in the simulation model to the previous usage. The hydraulic diagram of an EHA is shown in Figure 3.1.

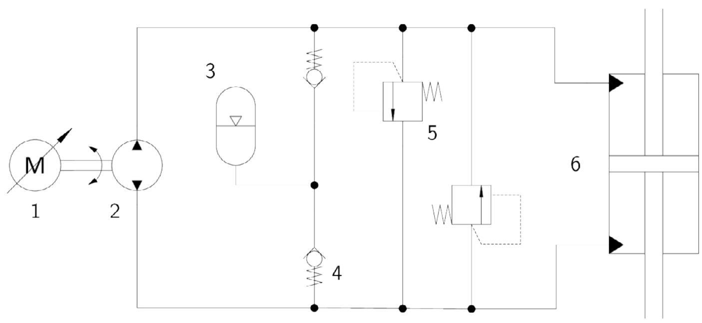

Figure 3.1: EHA hydraulic diagram. 1. Electric motor. 2. Hydraulic pump. 3. Accumulator. 4. Check-valves. 5. Pressure-relief valves. 6. Double-acting cylinder.

The hydraulic pump is modeled as an external gear pump. The outflow of the pump is modeled with Schlösser's loss coefficient model [28]

$$Q_A = V_p n - C_{sl}\frac{V_p(p_{h,A} - p_{h,B})}{2\pi\nu} - C_{st}V_p^{\frac{2}{3}}\sqrt{\frac{2(p_{h,A} - p_{h,B})}{\rho}} - C_{se}p_{h,A}, \tag{33}$$

where V_p is the volumetric displacement, n is the rotational speed, C_{sl} is the laminar slip coefficient, $p_{h,A}$ and $p_{h,B}$ are the hose pressures, ν is the dynamic viscosity, C_{st} is the turbulent slip coefficient, ρ is the oil density, and C_{se} is the external leakage coefficient.

During the system operation, the performance of the actuator gradually deteriorates. This degradation can be represented by certain actuator parameters. In this study, the slip coefficients C_{sl} and C_{st} are utilized as hidden variables to characterize the degradation of the pump. This is motivated by the fact that internal leakage increases over time [29]. This choice is illustrative as other parameters could also be used. Based on Equation (1), the hidden degradation process is modelled as

$$C_{sl}(t) = C_{sl}(0) + \int_0^t \lambda_1|n(\tau)| + \lambda_2\left|\frac{d}{d\tau}n(\tau)\right| \, d\tau + \sigma B_1(t), \tag{34}$$

$$C_{st}(t) = C_{st}(0) + \int_0^t \lambda_1|n(\tau)| + \lambda_2\left|\frac{d}{d\tau}n(\tau)\right| \, d\tau + \sigma B_2(t), \tag{35}$$

where λ_i is the degradation rate coefficient. Here, it is assumed that both slip coefficients increase by the same proportion, but the Brownian motion is different. It is also assumed that the amount of degradation per unit of time is proportional to the amplitude of the rotational speed and the rotational acceleration. This assumption reflects the fact that stress is usage-dependent and increases with higher rotational speed and fast changes between operation points. Therefore, increasing controller aggressiveness can increase peak acceleration, but may still reduce cumulative degradation if it shortens transients and reduces the time spent at elevated rotational speed. The resulting effect is not necessarily monotonic in k_p and depends on the duty cycle and the coefficients of the speed- and acceleration-dependent terms.

In the EKF, a lumped parameter model for internal leakage

$$Q_A = V_p n - \hat{\phi}(p_{h,A} - p_{h,B}) - C_{se}p_{h,A}, \tag{36}$$

was utilized as the measurement function in Equation (6). This formulation allows for a straightforward definition of the failure threshold based on the operation requirements of the cylinder. For the simulations, the failure threshold was set to $\phi_f = 4 \cdot 10^{-12}\ (m^3/s)/Pa$. It is assumed that the volumetric displacement and the external leakage coefficient are known, while flow, rotational speed, and pressures are measured.

The simulation model parameters are summarized in

Table 1. The table presents only the parameters that differ from the previous publication [27]. The position reference and load forces are also identical to the previous publication. These were repeated until the degradation reached the specified failure threshold in the simulation.

Table 1: EHA simulation model parameters compared to previous publication [27]

Parameter	Symbol	Value
Pump displacement	V_p	$1.2732 \cdot 10^{-6}\ m^3/rad$
Initial laminar slip coeff.	$C_{sl}(0)$	$5 \cdot 10^{-9}$
Initial turbulent slip coeff.	$C_{st}(0)$	10^{-11}
External leakage coeff.	C_{se}	10^{-13}
Rot. speed degradation rate coeff.	λ_1	$2 \cdot 10^{-11}$
Rot. accel. degradation rate coeff.	λ_2	$8 \cdot 10^{-12}$
Diffusion coefficient	σ	10^{-9}
Dynamic viscosity	ν	$0.03\ Pa \cdot s$
Bulk modulus (cylinder)	β_{cyl}	$1200 \cdot 10^6\ Pa$
Bulk modulus (hose)	β_{hose}	$400 \cdot 10^6\ Pa$

The EHA position is controlled by a 2DOF-PID controller. The control signal is calculated according to Equations (24)–(27). The parameters of the controller are presented in Table 2. The controller gain is adjusted with the previously described adjustment mechanism. The parameters of the prognostics and health monitoring system are presented in Table 3.

Table 2: PID controller parameters

Parameter	Symbol	Value
Nominal gain	k_p	$4000\ (rad/s)/m$
Integral time	t_i	$1.6000\ s$
Derivative time	t_d	$0.3750\ s$
Filter time constant	τ_f	$0.0250\ s$
Proportional reference weight	b	0.5
Derivative reference weight	c	0
Controller sampling time	t_s	$0.01\ s$

Table 3: Prognostics and health monitoring system parameters

Parameter	Symbol	Value
EKF sampling time	$t_{s,ekf}$	$0.05\ s$
EKF state covariance	Σ_w	$\begin{bmatrix} 0.0006 & 0.0179 \\ 0.0179 & 0.7170 \end{bmatrix} \cdot 10^{-16}$

EKF measurement covariance	Σ_v	$2 \cdot 10^{-5}$
Buffer time	t_{buf}	$200\ s$
Adj. mech. evaluation step	t_{eval}	$400\ s$
Controller gain, lower bound	$k_{p,min}$	$1000\ (rad/s)/m$
Controller gain, upper bound	$k_{p,max}$	$10000\ (rad/s)/m$
Cost function tracking weight	w_1	$1/m^2s$
Cost function health weight	w_2	$1/s^2$

4. RESULTS

The deterioration of the gear pump in an EHA is inevitable but can be delayed by adjusting the controller parameters. To illustrate this application of the predicted RUL and adjustment mechanism, the proposed method is applied to the EHA position control system. The simulations were conducted with MATLAB Simulink in accelerated conditions, i.e., the coefficients of Equations (34) and (35) are greatly exaggerated. This leads to the pump failing in about 30 minutes rather than thousands of hours. In the simulations the EHA is supposed to operate for longer than $t_{RUL,req} = 1850\ s$ with the probability $p = 95\%$. The adjustment mechanism evaluation times were set $400\ s$ apart.

Figure 4.1 shows the degradation evolution for the baseline system and the system with the adjustment mechanism enabled. The points where the controller gain is adjusted are highlighted with dashed grey lines. After the first adjustment at $t = 400\ s$, it is evident that the degradation rate slows down compared to the baseline. Although the gain increase can raise peak acceleration during reference transitions, the net degradation slows because Equations (34) and (35) depend on the integrated rotational speed/acceleration. Under this duty cycle the updated gain reduces the duration and average level of the stress terms. In the baseline simulation, $t_{RUL,req}$ was broken with 25 seconds. The adjustment mechanism successfully extended the RUL of the system by 46 seconds, which fulfilled the operation time requirement.

As an additional reference, a fixed-gain simulation was conducted by setting the proportional gain k_p to $8000\ (rad/s)/m$. This was done to maximize useful life for this specific duty cycle and model parameterization. In this case, the achieved useful life increased to approximately $2060\ s$, compared with $1825\ s$ for the nominal fixed-gain baseline and $1871\ s$ for the gain-updated case. This result should be interpreted as scenario specific as the optimal fixed gain depends on the duty cycle, load, and modeling uncertainty, and therefore serves as an upper bound rather than a generally applicable tuning.

In Figure 4.2, the adjusted controller gain of the PID controller is shown with the constant gain of the baseline simulation. The effect of changing the controller gain to the squared control error is illustrated in Figure 4.3. At the first adjustment time, there is a small increase in the control error caused by the sudden change of controller gain. Figure 4.3 also shows that the peaks of the control error increase over time. This is caused by the deterioration of the pump, which causes it to produce less flow and in turn makes it more difficult to follow the changing reference points. The error peaks of the adjusted controller are slightly smaller, caused by the cost function (31) including the ISE in the optimization.

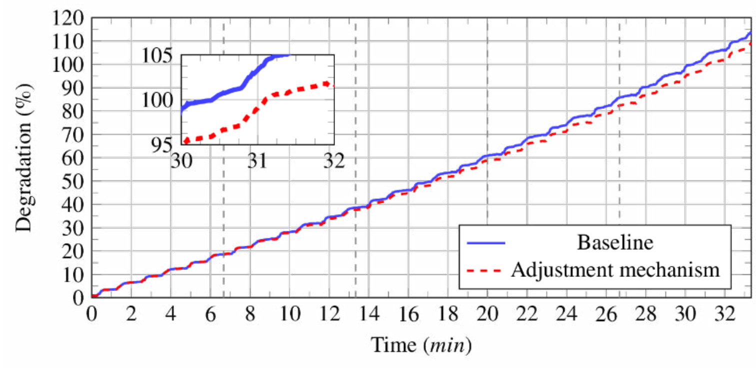

Figure 4.1: Evolution of estimated degradation in accelerated simulation conditions.

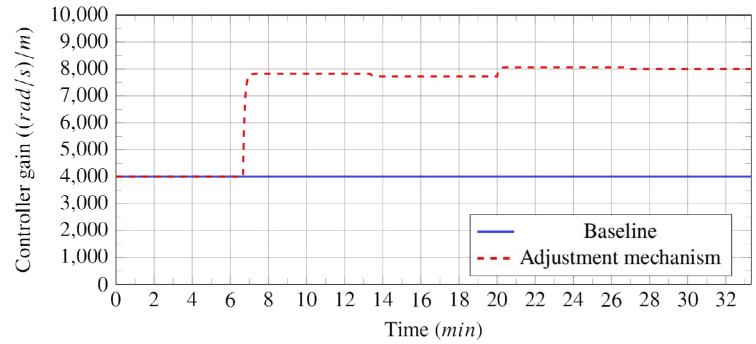

Figure 4.2: Proportional gain in the baseline test and under the adjustment mechanism.

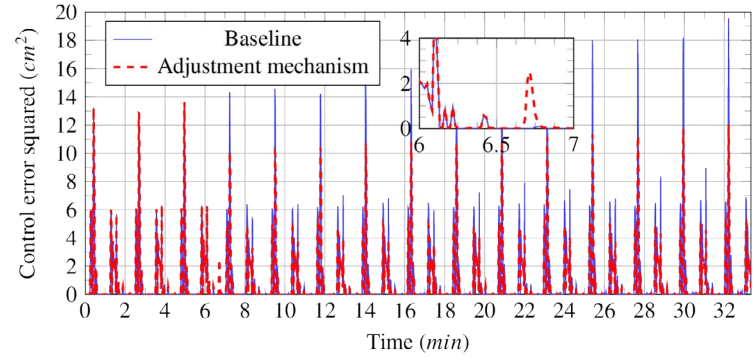

Figure 4.3: Squared control error for the two scenarios with zoomed in section of the first adjustment time.

From Figure 4.2, it is evident that after the first adjustment, there is no need for the subsequent adjustments. This is mostly due to the assumption of linear degradation evolution holding very well for the whole simulation, which is caused by two main factors. Firstly, the cyclic nature of the position reference and load signals utilized in the simulation cause the degradation to increase almost the same amount per cycle. This is somewhat offset by the increased leakage flow for which the controller must compensate by increasing the rotational speed, which in turn accelerates the degradation towards the end of the simulation. Secondly, the chosen degradation models, i.e., Equations (34) and (35), increase the degradation speed independently from the age/degradation of the component. In real systems this might not be true, as the degradation speed of the component can be considerably faster near the end of its life.

5. CONCLUSION

This paper introduced a degradation-aware adjustment method for a PID-controller in an EHA system. An extended Kalman filter-based degradation estimator was combined with an inverse-Gaussian RUL formulation and a simple ridge model linking the control effort to the degradation rate. These were used in a cost function that trades tracking performance against a soft health constraint. The approach targets systems where maintenance is challenging and controller retrofits are preferred over a full health-aware control redesign.

Simulations with an EHA model under accelerated degradation showed that the proposed mechanism met the mission-time requirement at the specified survival-probability level. The nominal fixed-gain baseline achieved a useful life of $1825\ s$, whereas the system with the proposed adjustment mechanism increased the useful life to $1871\ s$ with only a modest transient increase in control error. As an additional benchmark, selecting the near scenario optimal fixed gain increased the useful life to approximately $2060\ s$. This gap indicates that, for a static and known duty cycle, offline tuning can outperform delayed online adjustment. Accordingly, the proposed mechanism is primarily aimed at settings where the best tuning is not known beforehand and/or operating conditions evolve over time.

The practical implication is that existing PID-controlled electro-hydraulic installations can gain significant life-extension potential with minimal architectural change. The method can be implemented as a supervisory layer (potentially cloud-based) that periodically re-tunes a small set of controller parameters using rotational speed, flow, and pressure data. While speed feedback and pressure are commonly available, direct flow sensing typically is not and may require added instrumentation or a validated virtual-sensing alternative. For practitioners, this provides a low-intrusion pathway to improve availability and maintenance planning by aligning controller aggressiveness with the remaining mission time, provided the required measurements are available.

This study has limitations worth noting. The results are based on simulations with accelerated degradation and simplified Wiener-type models whose parameters and threshold selection impact RUL accuracy. The controller adjustment tuned only the controller gain, and other PID parameters were kept fixed. The simulated duty cycle was cyclic, which favored near-linear degradation over the horizon, and may not generalize to all duty cycles or late-life behaviors where degradation can accelerate.

Future work should include experimental validation on hardware and the identification of more detailed degradation mechanisms and thresholds to improve model fidelity. In addition, the supervisory strategy should be evaluated under dynamic duty cycles, including varying loads and reference trajectories, to quantify robustness and to determine when online supervision provides a clear advantage over a priori fixed-gain tuning. Robust estimation under changing operating conditions, adaptive evaluation schedules, and integration with maintenance planning tools are also recommended to broaden applicability and reliability.

ACKNOWLEDGMENT

We acknowledge the financial support of the Finnish Ministry of Education and Culture through the Intelligent Work Machines Doctoral Education Pilot Program (IWM VN/3137/2024-OKM-4).

6. REFERENCES

[1] I. Bejaoui, D. Bruneo, and M. G. Xibilia, “A Data-Driven Prognostics Technique and RUL Prediction of Rotating Machines Using an Exponential Degradation Model,” in *2020 7th International Conference on Control, Decision and Information Technologies (CoDIT)*, June 2020, pp. 703–708. doi: 10.1109/CoDIT49905.2020.9263930.

[2] A. Dahal, Y. Li, S. Khanal, S. G. Niazi, and H.-Z. Huang, “Remaining useful life prediction of induction motor based on hybrid temporal convolution neural network,” in *14th International Conference on Quality, Reliability, Risk, Maintenance, and Safety Engineering (QR2MSE 2024)*, July 2024, pp. 1280–1285. doi: 10.1049/icp.2024.3616.

[3] Cun Shi, Shaoping Wang, Xingjian Wang, and Jun Wang, “Remaining useful life prediction based on particle filtering for high-speed pump in load sensing electro-hydrostatic actuator,” in *CSAA/IET International Conference on Aircraft Utility Systems (AUS 2018)*, Guiyang, China: Institution of Engineering and Technology, 2018, p. 238 (6 pp.)-238 (6 pp.). doi: 10.1049/cp.2018.0312.

[4] Y. Zhang, S. Wang, C. Zhang, and R. Chen, “Physics-Based Machine Learning Hydraulic Piston Pump Performance Degradation and Prognostics,” in *2023 7th International Conference on System Reliability and Safety (ICSRS)*, Bologna, Italy: IEEE, Nov. 2023, pp. 389–394. doi: 10.1109/ICSRS59833.2023.10381233.

[5] M.-S. Lee, T. A. Shifat, and J.-W. Hur, “Kalman Filter Assisted Deep Feature Learning for RUL Prediction of Hydraulic Gear Pump,” *IEEE Sens. J.*, vol. 22, no. 11, pp. 11088–11097, June 2022, doi: 10.1109/JSEN.2022.3167926.

[6] R. Guo, Y. Li, L. Zhao, J. Zhao, and D. Gao, “Remaining Useful Life Prediction Based on the Bayesian Regularized Radial Basis Function Neural Network for an External Gear Pump,” *IEEE Access*, vol. 8, pp. 107498–107509, 2020, doi: 10.1109/ACCESS.2020.3001013.

[7] P. Liu, S. He, K. Gao, G. Yang, J. Zou, and L. Ye, “Prediction of hydraulic pumps remaining useful life based on LSTM and Transform with dual self-attention,” in *2023 IEEE Intl Conf on Parallel & Distributed Processing with Applications, Big*

Data & Cloud Computing, Sustainable Computing & Communications, Social Computing & Networking (ISPA/BDCloud/SocialCom/SustainCom), Wuhan, China: IEEE, Dec. 2023, pp. 824–831. doi: 10.1109/ISPA-BDCloud-SocialCom-SustainCom59178.2023.00140.

[8] C. Li, J. Wang, X. Li, X. Li, J. Xu, and D. Mba, “PGMTKD: A Physics-Guided Multi-Teacher Knowledge Distillation network for external gear pump onboard fault diagnosis with missing modality,” *Mech. Syst. Signal Process.*, vol. 239, p. 113296, Oct. 2025, doi: 10.1016/j.ymssp.2025.113296.

[9] W. Xu, Z. Wang, Z. Zhou, C. Sun, R. Yan, and X. Chen, “Wear state assessment of external gear pump based on system-level hybrid digital twin,” *Mech. Syst. Signal Process.*, vol. 209, p. 111123, Mar. 2024, doi: 10.1016/j.ymssp.2024.111123.

[10] T. Escobet, V. Puig, and F. Nejjari, “Health Aware Control and model-based Prognosis,” presented at the 2012 20th Mediterranean Conference on Control and Automation, MED 2012 - Conference Proceedings, 2012, pp. 691–696. doi: 10.1109/MED.2012.6265718.

[11] S. A. Nahian, D. Q. Truong, P. Chowdhury, D. Das, and K. K. Ahn, “Modeling and fault tolerant control of an electro-hydraulic actuator,” *Int. J. Precis. Eng. Manuf.*, vol. 17, no. 10, pp. 1285–1297, Oct. 2016, doi: 10.1007/s12541-016-0153-2.

[12] L. Liao and F. Köttig, “Review of Hybrid Prognostics Approaches for Remaining Useful Life Prediction of Engineered Systems, and an Application to Battery Life Prediction,” *IEEE Trans. Reliab.*, vol. 63, no. 1, pp. 191–207, Mar. 2014, doi: 10.1109/TR.2014.2299152.

[13] Y. Hu, S. Liu, H. Lu, and H. Zhang, “Remaining Useful Life Model and Assessment of Mechanical Products: A Brief Review and a Note on the State Space Model Method,” *Chin. J. Mech. Eng.*, vol. 32, no. 1, p. 15, Feb. 2019, doi: 10.1186/s10033-019-0317-y.

[14] J. Thuillier, M. S. Jha, M. Galeotta, and D. Theilliol, “Control reconfiguration strategies for Remaining Useful Life extension,” *IFAC-Pap.*, vol. 55, no. 34, pp. 114–119, Jan. 2022, doi: 10.1016/j.ifacol.2022.11.317.

[15] J. Matias and J. Jäschke, “Balancing production maximization and equipment degradation: Experimental application of a health-aware controller,” *Control Eng. Pract.*, vol. 156, p. 106193, Mar. 2025, doi: 10.1016/j.conengprac.2024.106193.

[16] E. Kipchirchir, M. H. Do, J. G. Njiri, and D. Söffker, “Prognostics-based adaptive control strategy for lifetime control of wind turbines,” *Wind Energy Sci.*, vol. 8, no. 4, pp. 575–588, 2023, doi: 10.5194/wes-8-575-2023.

[17] M. Zagorowska, O. Wu, J. R. Ottewill, M. Reble, and N. F. Thornhill, “A survey of models of degradation for control applications,” *Annu. Rev. Control*, vol. 50, pp. 150–173, Jan. 2020, doi: 10.1016/j.arcontrol.2020.08.002.

[18] R. D. de Oliveira and J. Jäschke, “Integration of time scales in health-aware control,” presented at the IFAC-PapersOnLine, 2024, pp. 222–227. doi: 10.1016/j.ifacol.2024.08.340.

[19] M. Kumar, "A survey on electro hydrostatic actuator: Architecture and way ahead," *Mater. Today Proc.*, vol. 45, pp. 6057–6063, Jan. 2021, doi: 10.1016/j.matpr.2020.10.049.

[20] Z. Zhang, X. Si, C. Hu, and Y. Lei, "Degradation data analysis and remaining useful life estimation: A review on Wiener-process-based methods," *Eur. J. Oper. Res.*, vol. 271, no. 3, pp. 775–796, Dec. 2018, doi: 10.1016/j.ejor.2018.02.033.

[21] H. Wang, X. Ma, and Y. Zhao, "An improved Wiener process model with adaptive drift and diffusion for online remaining useful life prediction," *Mech. Syst. Signal Process.*, vol. 127, pp. 370–387, July 2019, doi: 10.1016/j.ymssp.2019.03.019.

[22] X. Si, Z. Ren, X. Hu, C. Hu, and Q. Shi, "A Novel Degradation Modeling and Prognostic Framework for Closed-Loop Systems With Degrading Actuator," *IEEE Trans. Ind. Electron.*, vol. 67, no. 11, pp. 9635–9647, Nov. 2020, doi: 10.1109/TIE.2019.2952828.

[23] M.-L. T. Lee and G. A. Whitmore, "Threshold Regression for Survival Analysis: Modeling Event Times by a Stochastic Process Reaching a Boundary," *Stat. Sci.*, vol. 21, no. 4, Nov. 2006, doi: 10.1214/088342306000000330.

[24] S. Särkkä, *Bayesian filtering and smoothing*. in Institute of Mathematical Statistics textbooks, no. 3. Cambridge, U.K. ; New York: Cambridge University Press, 2013.

[25] A. K. M. E. Saleh, M. Arashi, and B. M. G. Kibria, *Theory of ridge regression estimation with applications*. Hoboken, NJ: John Wiley & Sons, 2019.

[26] K. J. Åström and T. Hägglund, *Advanced PID control*. Research Triangle Park, NC: ISA - The Instrumentation, Systems, and Automation Soc, 2006.

[27] S. Käki, V. P. Singh, M. Huova, and T. Minav, "Health Aware Control Design for Extending Remaining Useful Life of Electro-Hydrostatic Actuator Based Steering," in *The 19th Scandinavian International Conference on Fluid Power, SICFP'25*, Linköping University, Sweden: River Publishers, 2025, pp. 176–186. doi: 10.13052/rp-9788743808251A17.

[28] M. Torrent, P. J. Gamez-Montero, and E. Codina, "Parameterization, Modeling, and Validation in Real Conditions of an External Gear Pump," *Sustainability*, vol. 13, no. 6, p. 3089, Mar. 2021, doi: 10.3390/su13063089.

[29] Y. Duensing, A. Merkel, and K. Schmitz, "Degradation Identification of an EHA Piston Pump by Analysis of Load-Holding States," *Int. J. Fluid Power*, pp. 273–290, July 2024, doi: 10.13052/ijfp1439-9776.2528.

Biographies

Simo Käki graduated with the M.Sc. (Tech.) degree in automation technology from Tampere University, Finland, in 2024. Currently he is a Doctoral Researcher at Innovative Hydraulics and Automation (IHA), Tampere University, Finland. His research focuses on advanced control of electro-hydraulic systems and extension of remaining useful life of components with intelligent control.

Mikko Huova received the doctoral degree at Tampere University of Technology, Finland, in 2015. Currently he is a Senior Research Fellow at IHA lab of Tampere University, Finland. His research focuses on advanced control, multi-pressure systems, and energy efficient digital hydraulic systems of heavy-duty mobile machines.

Tatiana Minav has over 18 years of experience improving the efficiency and sustainability of off-road mobile working machines and innovatively combining signal processing, electrical and mechanical engineering. Since 2019 she has been an associate professor (tenured) in the largest Finnish fluid power laboratory at Tampere University, which specializes in off-road machinery, efficiency, powertrain, fluid power and automation-related topics. Professor Minav has authored ca 180 international scientific publications.